Nucleic Acids Research, 1999, Vol. 27, No. 2 555–561

The crystal structure of the RNA/DNA hybrid r(GAAGAGAAGC)·d(GCTTCTCTTC) shows significant differences to that found in solution

Graeme L. Conn[+], Tom Brown and Gordon A. Leonard[1,*]

Department of Chemistry, University of Southampton, Southampton SO17 1BJ, UK and [1]Joint ESRF/EMBL Structural Biology Group, European Synchrotron Radiation Facility, BP 200, F-38034 Grenoble Cedex, France

Received September 14, 1998; Revised and Accepted November 10, 1998

NDB accession no. AH0001

ABSTRACT

The crystal structure of the RNA/DNA hybrid r(GAAGAGAAGC)·d(GCTTCTCTTC) has been solved and refined at 2.5 Å resolution. The refinement procedure converged at R = 0.181 for all reflections in the range 20.0–2.5 Å. In the crystal, the RNA/DNA hybrid duplex has an A′ conformation with all but one of the nucleotide sugar moieties adopting a C3′-*endo* (N) conformation. Both strands in the double helix adopt a global conformation close to the A-form and the width of the minor groove is typical of that found in the crystal structures of other A-form duplexes. However, differences are observed between the RNA and DNA strands that make up the hybrid at the local level. In the central portion of the duplex, the RNA strand has backbone α, β and γ torsion angles that alternate between the normal *gauche*[−]/*trans*/*gauche*[+] conformation and an unusual *trans*/*trans*/*trans* conformation. Coupled with this so-called 'α/γ flipping' of the backbone torsion angles, the distance between adjacent phosphorous atoms on the RNA strand systematically varies. Neither of these phenomena are observed on the DNA strand. The structure of the RNA/DNA hybrid presented here differs significantly from that found in solution for this and other sequences. Possible reasons for these differences and their implications for the current model of RNase H activity are discussed.

INTRODUCTION

RNA/DNA hybrid formation is a crucial step in important biological processes such as transcription and the replication of DNA (1,2), as well as in the 'antisense' approach of artificially arresting gene expression (3). When RNA/DNA hybrids are formed, the RNA strand becomes a substrate for the enzyme RNase H. RNase H does not hydrolyse RNA when either single or double stranded (4) but in general displays little sequence specificity in the site of hydrolysis of the RNA strand of a hybrid duplex. In the absence of any crystal or solution structures of RNase H–hybrid complexes, quite how the enzyme distinguishes pure RNA and RNA/DNA hybrid duplexes is unclear. Analyses of the crystal structures of chimeric RNA/DNA hybrids indicate that they are (like RNA duplexes) almost pure A-form in conformation (5,6) and give no hint as to how this distinction between the two types of duplex could be effected. In contrast, NMR analysis of the structures of RNA/DNA hybrids in solution suggests that the DNA strands of these duplexes have helical conformations intermediate between the A- and B-forms (7–13). It has been proposed that the non-standard conformation of the resulting duplexes provides a mechanism for RNase H to selectively recognise and hydrolyse the RNA strand of a hybrid duplex (7–9). It has also been reported that the stability of rR·dY hybrids is greater than that of rY·dR (i.e. that hybrids in which the RNA strand consists entirely of purines are more stable than those where it consists entirely of pyrimidines) (14–17). Solution studies (7) of a series of duplexes containing purine-rich (GAAGAGAAGC) and pyrimidine-rich (GCTTCTCTTC or GCUUCUCUUC) RNA or DNA strands have confirmed this with the thermodynamic stability of the duplexes being rR·rY > rR·dY > dR·dY > dR·rY. The relative stabilities of the two RNA/DNA hybrids in the series has been explained by the fact that while both the duplexes have double helical structures intermediate between the A- and B-forms, that of rR·dY is closer to A-form than that of dR·dY. The intermediate structure of rR·dY also appears to explain its relative lack of stability in comparison with the rR·rY duplex in which both strands adopt the A conformation (8). In order to further investigate this phenomenon we set out to solve the crystal structures of all four duplexes in the above series. Here we report the results of our single crystal X-ray analysis of r(GAAGAGAAGC)·d(GCTTCTCTTC) and we compare the crystal structure of the RNA/DNA hybrid with that found in solution. Significant differences are observed between the two and these may have implications for current models of the mode of recognition of such hybrids by RNase H.

MATERIALS AND METHODS

Chemical synthesis and crystallisation

r(GAAGAGAAGC) and d(GCTTCTCTTC) were prepared as described previously (7) with the exception that the primary

*To whom correspondence should be addressed. Tel: +33 4 76 88 23 94; Fax: +33 4 76 88 27 07; Email: leonard@esrf.fr

[+]Present address: Department of Chemistry, Johns Hopkins University, 3400 North Charles Street, Baltimore, MD 21218, USA

purification was by strong anion exchange HPLC (Dionex Nucleopac-PA 100) using a gradient of ammonium chloride (0.0–1.0 M) in 50 mM Tris buffer, pH 7.0. After desalting on Sephadex G-10, the oligonucleotides were lyophilized from water and redissolved in 10 mM sodium cacodylate buffer, pH 6.5, containing 1 mM spermine hydrochloride. Equimolar concentrations of each strand, as determined from their measured extinction coefficients (18), were mixed to give a final duplex concentration of 1 mM. Crystallisation conditions (19) were screened in 4 µl hanging drops containing 2 µl each of the hybrid duplex and crystallisation solutions, equilibrated against 500 µl of the crystallisation solution. Crystals were obtained in 25 out of the 48 conditions used in the screen. The crystals used for data collection grew in 1–2 days from 50 mM HEPES buffer (pH 7.0) containing 5% PEG4000, 200 mM ammonium acetate and 150 mM magnesium acetate.

X-ray data collection, structure solution and refinement

A crystal of the RNA/DNA hybrid was mounted in a Lindemann capillary in the presence of a small amount of the crystallisation drop mother liquor and was used for X-ray data collection. Sixty 3° oscillation images were measured using the Princeton-ESRF CCD camera on beamline BM14 at the ESRF at λ = 0.763 Å. Correction of the raw CCD images was performed using the program FIT2D (A.P.Hammersly, personal communication) and autoindexing and data processing with DENZO (20). The reflections were exceptionally wide in the ϕ dimension. However, all attempts to model this using post-refinement in the program SCALEPACK (20) were unsuccessful and the data was processed assuming a crystal mosaicity of 1° with no post-refinement or addition of partial reflections during the scaling procedure. This resulted in a data set for structure solution and refinement containing 1881 unique reflections in the resolution range 30.0–2.5 Å with R_{sym} = 5.6%. The redundancy in the data set is 4.06 and the data is 86.6% complete within the stated resolution range.

The crystals of the RNA/DNA hybrid belong to the orthorhombic crystal system with unit cell dimensions *a* = 25.70 Å, *b* = 45.85 Å, *c* = 47.75 Å and space group $P2_12_12_1$. From a search of the Nucleic Acid Database (21), the structure of the RNA/DNA hybrid appeared to be quasi-isomorphous with several other DNA and chimeric DNA/RNA duplexes which crystallize with similar unit cell dimensions in the same space group. The coordinates of one of these, the DNA decamer $d(CCCGGCCGGG)_2$ (22), were arbitrarily chosen as a search model for molecular replacement calculations. These were performed using the program ULTIMA (23). An initial rotation/translation search was carried out using data in the resolution range 25.0–8.0 Å. Subsequent rigid body refinement of the top 60 potential solutions was then carried out in a step-wise fashion using data in the resolution ranges 25.0–8.0, 25.0–6.0, 8.0–5.0, 8.0–4.0 and, finally, 8.0–3.0 Å. The choice of best solution was not obvious. However, that with the best (F_{obs}, F_{calc}) correlation coefficient gave an R factor of 0.53 and when examined on a computer graphics system appeared to have reasonable crystal packing. This model was therefore chosen for further refinement.

After first assigning an R_{free} subset of reflections in the data (24), initial refinement was first performed with the program X-PLOR (25). The stereochemical restraints employed (and the weights associated with them) were those defined by Parker *et al.* (26) except that those torsion angles pertaining to sugar pucker were not restrained to specific values. Additionally, all atoms in the model resulting from the molecular replacement procedure described above were assigned a temperature factor of 16.0 Å^2. An initial round of positional refinement using data in the range 25.0–2.5 Å reduced R_{work} and R_{free} to 0.37 and 0.50 from initial values of 0.56 and 0.61, respectively. At this stage both electron density ($2F_{obs} - F_{calc}$, α_{calc}) and difference density ($F_{obs} - F_{calc}$, α_{calc}) maps were examined to see if the model could be improved by manual fitting prior to further refinement. The maps were of excellent quality allowing immediate assignment of the correct base sequence and the positioning of all the O2′ oxygen atoms for the ribose moieties on the RNA strand and the thymine 5-methyl carbon atoms on the DNA strand. This improved model gave initial values for R_{work} and R_{free} of 0.36 and 0.37 as calculated in X-PLOR which after one further round of positional refinement were reduced to 0.25 and 0.27, respectively. Refinement was continued with the program REFMAC (27). using the same R_{free} set. Here, individual isotropic temperature factors were also refined and no restraints were applied to any torsion angle. Six cycles of refinement reduced R_{work} and R_{free} to values of 0.184 and 0.230, respectively. Both electron density and difference density maps were then examined in order to check the fit of the model to the density and to identify potential solvent molecules in the structure. Surprisingly, few of these could be located. Although there were a number of peaks in the difference density map only nine of these coincided with spherical density in the electron density map, even when it was examined at a 0.75σ contour level. These nine solvents were included in the model. At this stage the R_{free} subset of data was dispensed with and a final round of refinement using all data (1867 reflections) in the resolution range 20.0–2.5 Å yielded a final value for the crystallographic R factor of 0.181. As can be seen from Figure 1, the fit of the final model to the final electron density map is excellent. The geometry of the final model is also good, with r.m.s deviations from ideality being 0.014 and 0.047 Å for bond and angle distances, respectively. Final refined coordinates and the observed structure factor data have been submitted to the NDB with accession no. AH0001.

RESULTS AND DISCUSSION

The molecular structure of r(GAAGAGAAGC)·d(GCTTCTCTTC)

The RNA/DNA hybrid is a double helix stabilized by 10 standard Watson–Crick base pairs with the nucleotides labelled in the 5′→3′ direction G1–C10 on the RNA strand and G11–C20 on the DNA strand (Fig. 2). The average helical parameters of the double helix, calculated using the program NEWHEL93 (R.E.Dickerson, UCLA), are 30.4° for helix rotation and 2.9 Å for helical rise. There are thus 11.8 nucleotides per full helical turn and the pitch of the helix is 34.2 Å. These values place the duplex firmly in the A family, although they are more consistent with an A′-RNA conformation rather than the ‘classical’ A-RNA (Table 1). As such, it would appear that the crystal structure of r(GAAGAGAAGC)·d(GCTTCTCTTC) is similar to that observed in fibres of poly(rR)·poly(dY) at low relative humidity (28). To the best of our knowledge this is the first single crystal structure determination of an A′ nucleic acid double helix. This system could therefore serve as a template for further investigations into the structures of A′ duplexes. Apart from the difference in global helical rotation

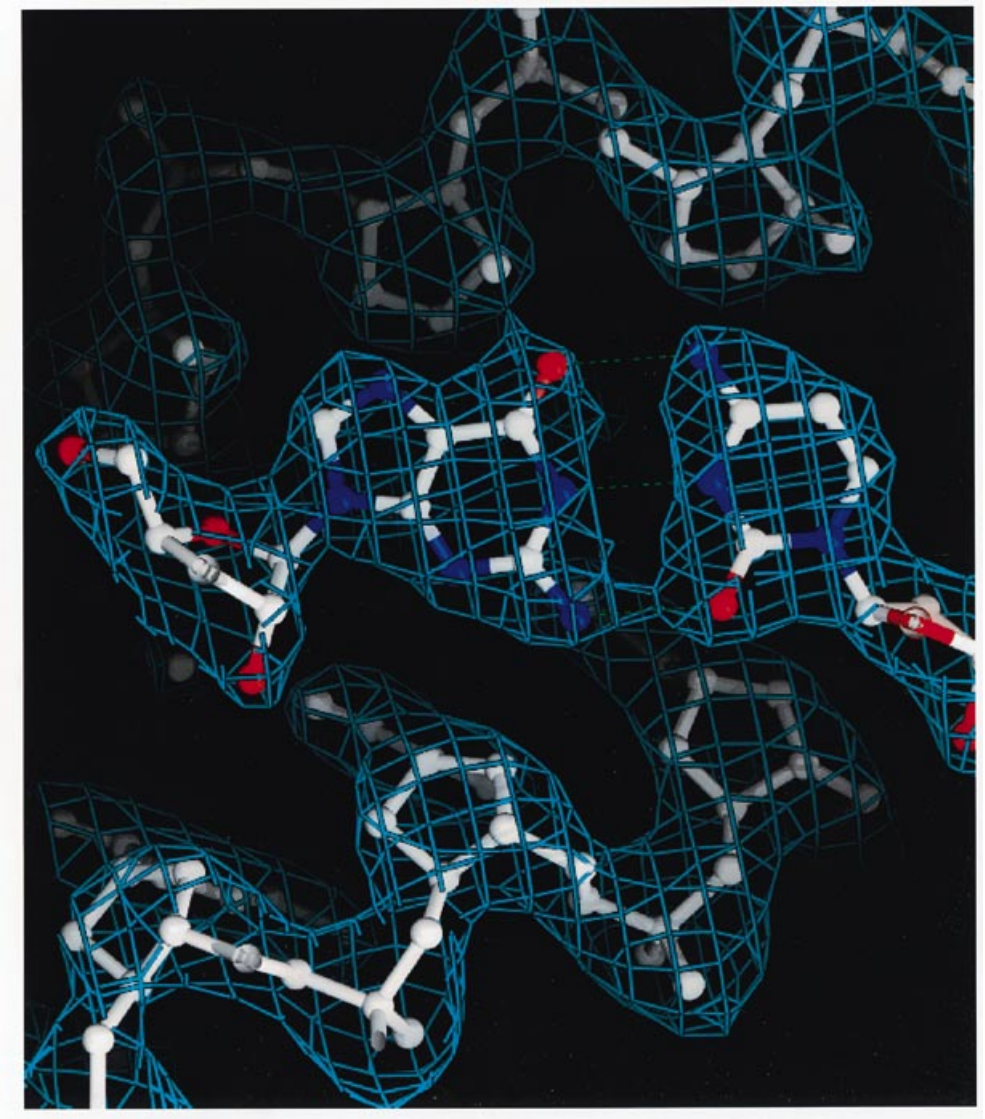

Figure 1. An example of the fit of the final refined model to the electron density ($2F_{obs} - F_{calc}$, α_{calc}) for the structure of (GAAGAGAAGC)·d(GCTTCTCTTC). Shown here are the rG(1)-dC(20) base pair with the sugar–phosphate backbones of symmetry-related molecules packing on both the major and minor groove sides of the base pair. In the base pair shown carbon atoms are coloured white, nitrogens blue, oxygens red and phosphorus atoms magenta. Atoms from symmetry-related molecules are either all white or all green. Figures 1 and 2 were produced using the program SPOCK (available at http://quorum.tamu.edu/jon/spock).

and rise, A′ duplexes have the same structural characteristics as true A-form double helices and this is the case here. Only the deoxyribose moiety of C20, which is clearly influenced by crystal packing contacts, does not adopt a sugar pucker close to C3′-*endo* (Fig. 3) and the local base pair and helical parameters of the duplex all cluster around typical A-form values (Table 1). The geometry of the minor groove (Fig. 4) of the RNA/DNA hybrid is also characteristic of crystalline A-form double helices. The average width of 9.8 Å is very close to the averages of those found in a survey of 19 A-type crystal structures in the NDB (data not shown) and, in the centre of the duplex, it is also close to the value of 11 Å found for the width of the minor groove from the fibre diffraction analysis of A-form helices (29). In contrast, it would appear that the major groove of the RNA/DNA hybrid double helix is somewhat different to that observed for A-form double helices from crystal or fibre diffraction analyses. For this duplex we can only measure the major groove width in two places, but even so the 'average' value of 8.4 Å for its width is clearly much larger than the value of 2.7 Å found in fibres or values of between 3 and 5 Å found for A-form decamer crystal structures in the NDB.

Despite the fact that both the RNA and DNA strands in the crystal structure of the hybrid appear to be globally in the A-form there are differences in the conformation of the two strands when they are compared at a local level. Given the chemical composition of the two strands, a valid comparison of their structures can only be made using the positions of the atoms on their sugar–phosphate backbones (O2′ atoms excluded). A least squares superposition of these results in a r.m.s. difference in atomic position of 1.24 Å. The largest deviations occur in the positions of the phosphate groups and the sizes of these deviations suggest that the backbone conformations of the two strands differ significantly. This impression is confirmed by an examination of the backbone

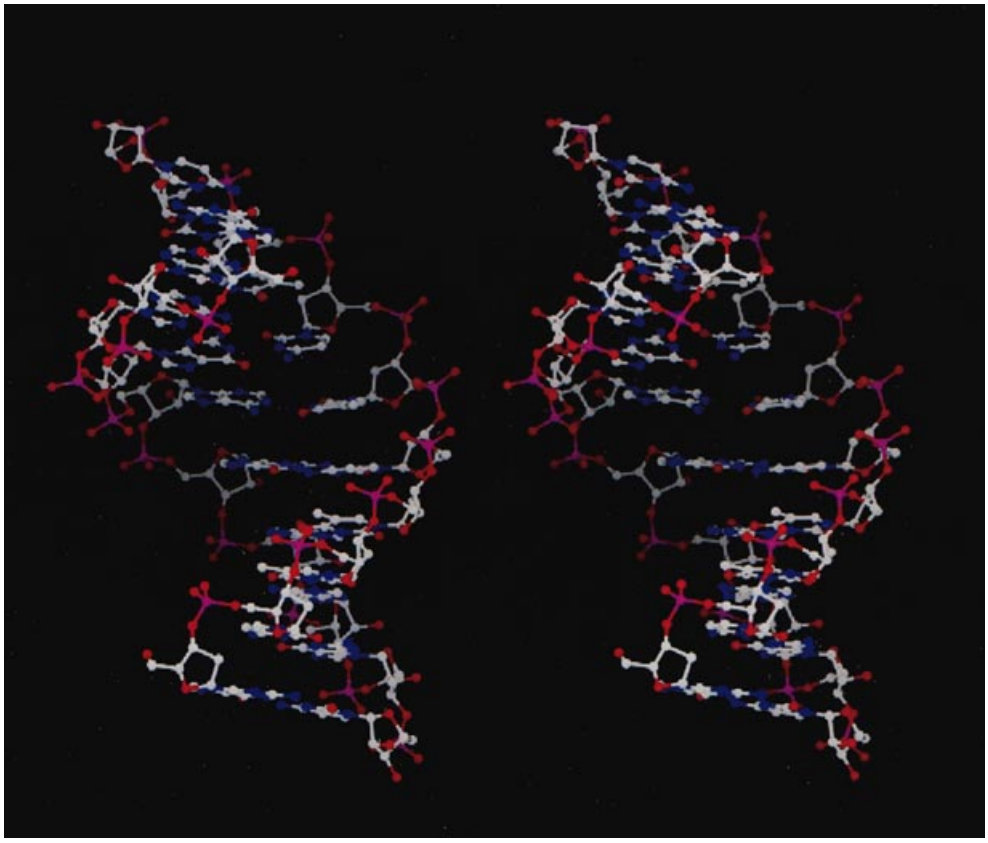

Figure 2. A stereoview of the final refined structure of r(GAAGAGAAGC)·d(GCTTCTCTTC). Atom colouring is as for Figure 1 and the view is into the minor groove of the duplex.

torsion angles adopted by the RNA/DNA hybrid as shown in Figure 3. In the DNA strand all the torsion angles are at values close to their preferred ones (29). In the RNA strand, however, nt 4, 6 and 8 have α, β and γ (αβγ) torsion angles which differ from the usual *gauche*$^-$/*trans*/*gauche*$^+$ (*gtg*) configuration with, in each case, the αβγ conformation being *trans*/*trans*/*trans* (*ttt*). These so-called 'α/γ flips' have been observed in the RNA strand of the average solution structures of both enantiomeric forms of d(GCTATAApsTGG)·r(CCAUUAUAGC) (12), the solution structure of d(CATTTGCATC)·d(GATGCAAATG) (30), the DNA strand of theoretical models of poly(dT)·poly(rA) (31), the crystal structure of an RNA double helix (32) and in several nucleic acid decamer structures as found in the NDB (21). In each of these cases, the *ttt* configuration is only observed for an isolated nucleotide (30,32) or the whole strand (31). Only for the RNA strands in the present structure, r(GAAGAGAAGC)·d(GCTTCTCTTC), and d(GCTATAApsTGG)·r(CCAUUAUAGC) (12) is this alternation between *gtg* and *ttt* conformations observed. The major effect of the αβγ *ttt* torsion angles is that the conformation of the nucleic acid sugar–phosphate backbone about the C4′-C5′ bond is now *ap* rather than the usual +*sc* (29). As a result, the P-O5′ and O5′-C5′ bonds of these nucleotides no longer point in towards the major groove of the duplex but now point almost in the opposite direction, with the O5′ atoms on the minor groove side of the duplex (Fig. 5). Hence, between residues 3 and 9 of the RNA strand there is an alternating change of the orientation of the C5-O5′ and O5′-P bonds with respect to the furanose rings (Fig. 2) which is not seen on the DNA strand.

A further difference between the two strands of the hybrid duplex is in the distance between adjacent phosphorous atoms. As can be seen from Figure 6, on the RNA strand, from the P(G4)–P(A5) distance onward, there is a systematic variation in the P–P distance with alternate stretching (average P–P distance 6.6 Å) and compression (average P–P distance 5.4 Å). In contrast, the distances between adjacent phosphorous atoms on the DNA strand are close to 5.9 Å, the value expected for A-form duplexes (29), with no systematic variation. This systematic alteration of backbone configuration cannot be simply explained by the base composition of the RNA strand. Although the *ap* backbone conformations do not occur at any particular base step, elongation of the P–P distance always follows a nucleotide with the *ap* backbone conformation, strongly indicating that the two phenomena are linked. Thus, both in this crystal and, on one occasion, in solution (12), systematic variations in the backbone configuration of the RNA strand of a RNA/DNA hybrid are observed that are not found in the complementary DNA strand or, significantly, in any pure RNA duplex. Additionally, in the present crystal structure this alternation in backbone configuration on the RNA strand is accompanied by a stretching and compression of the interphosphate distances.

Table 1. Selected base pair and base pair step parameters (twist and rise) for the r(GAAGAGAAGC)·d(GCTTCTCTTC) double helix as calculated using the program NEWHEL93 (R.E.Dickerson, UCLA)

Base pair	X_{dsp} (Å)	Inclination (°)	Tip (°)	Slide (Å)	Helical rise (Å)	Helical twist (°)
G1-C20	–3.6	14	3			
				–1.1	3.0	35
A2-T19	–4.1	15	4			
				–0.9	2.8	34
A3-T18	–4.0	15	–3			
				–2.1	2.6	28
G4-C17	–3.9	12	–8			
				–1.8	2.8	32
A5-T16	–5.8	7	–2			
				–1.8	3.4	28
G6-C15	–5.0	9	–1			
				–1.9	2.9	30
A7-T14	–4.8	14	3			
				–1.8	2.9	26
A8-T13	–4.0	17	–3			
				–1.8	2.5	30
G9-C12	–5.5	12	–10			
				–1.4	3.2	31
C10-G11	–6.3	6	–12			
Average	–4.7	12.1			2.9	30.4
A-DNA	–4.5	20			2.6	32.7
B-DNA	–0.14	–6			3.4	36.0
A-RNA	–	13			2.8	32.7
A′-RNA	–	14			3.0	30.0
r(R_{10})·d(Y_{10})	–3.3	6			2.9	33.7
r(R_{10})·r(Y_{10})	–5.2	8.1			2.6	31

For reference selected values of some of the above parameters are also shown for canonical nucleic acid double helical conformations (29) as well as those derived from the solution structures of r(GAAGAGAAGC)·d(GCTTCTCTTC) and r(GAAGAGAAGC)·r(GCTTCTCTTC) (7,8), which are denoted here as r(R_{10})·d(Y_{10}) and r(R_{10})·r(Y_{10}) respectively.

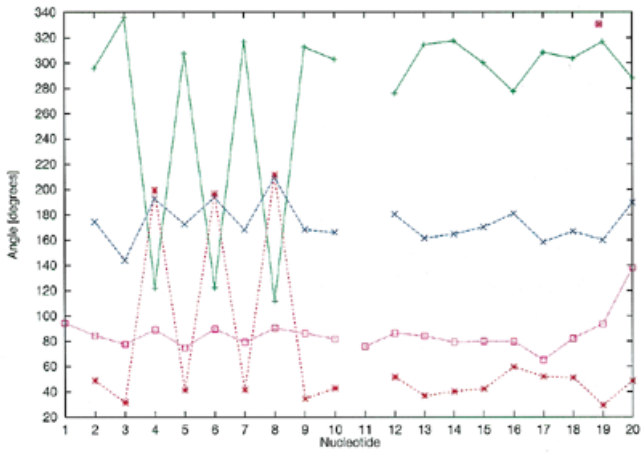

Figure 3. A plot of the backbone torsion angles α, β, γ and δ (shown in green, blue, red and magenta, respectively) for r(GAAGAGAAGC)·d(GCTTCTCTTC). All values of δ are close to that expected for C3′-*endo* (N) sugar puckering except for C20, where the observed C2′-*endo* (S) conformation is a result of crystal packing. Note the alternating αβγ *gtg*/*ttt* backbone conformation in the central part of the RNA strand.

Comparison with solution structures of RNA/DNA hybrids: implications for recognition by RNase H

Analysis of the solution structure of r(GAAGAGAAGC)·d(GCTTCTCTTC) using circular dichroism (CD) and ^{1}H and ^{31}P NMR spectroscopy (7,8) indicates that while globally it is close to the A-form, its conformation is in fact intermediate between the A- and B-forms, with the most significant deviations from A-form being on the DNA strand. In solution, the RNA strand is purely A-form but on the DNA strand there appears to be a C3′-*endo*/C2′-*endo* (N/S) equilibrium for the sugar moieties. An alternative interpretation of the NMR data is that the DNA sugars adopt a global O4′-*endo* (E) conformation (9,11). In either case, this results in the DNA strand, and therefore the double helix, having an average helical conformation intermediate between the A- and B-forms. This intermediate conformation is particularly apparent in the values observed for the inclination of the base pairs with respect to the helix axis, the dislocation of the base pairs from the helix axis (X_{dsp}) and the helical rise, all of which are between those found for A- and B-form double helices (Table 1). This intermediate global conformation has been observed in solution for several other RNA/DNA hybrids (9–13). It should be noted that this intermediate conformation has been observed, independently, by a number of different research groups and does not appear to depend on the different interpretations of sugar pucker used. This difference in global strand conformation is clearly not observed in the crystal structure of the RNA/DNA hybrid r(GAAGAGAAGC)·d(GCTTCTCTTC). The major consequence of this is that the minor groove is 1–2 Å wider in this crystal structure than in the solution structures of RNA/DNA hybrids (8,9,11,12).

It has been proposed (7–9), though not conclusively demonstrated, that the narrow minor groove observed in the solution structures of RNA/DNA hybrids is the critical factor in their recognition by RNase H. In this model the enzyme is able to bind across the minor groove simultaneously contacting both the RNA and DNA strands bringing the catalytic residues into the correct position. This simultaneous binding of the RNA and DNA strands by the enzyme appears to occur *in vitro* (33). The wider minor groove observed in the crystal structure of r(GAAGAGAAGC)·d(GCTTCTCTTC) is clearly less consistent with this hypothesis as it would require a conformational change to either the hybrid substrate, the RNase H or both to allow the simultaneous binding of both strands by the enzyme. There is, in fact, some evidence that conformational changes do occur in both the RNA/DNA hybrid and RNase H upon binding. In NMR studies, Oda *et al.* (34) have observed, upon duplex binding to RNase H, large changes in the chemical shifts of the amino acids Asp10, Asp70, His83 and Asn84. While the two former residues form part of the active site of the enzyme, the two latter do not and are located at the start of the so-called ‘basic protrusion’ (35; Fig. 2

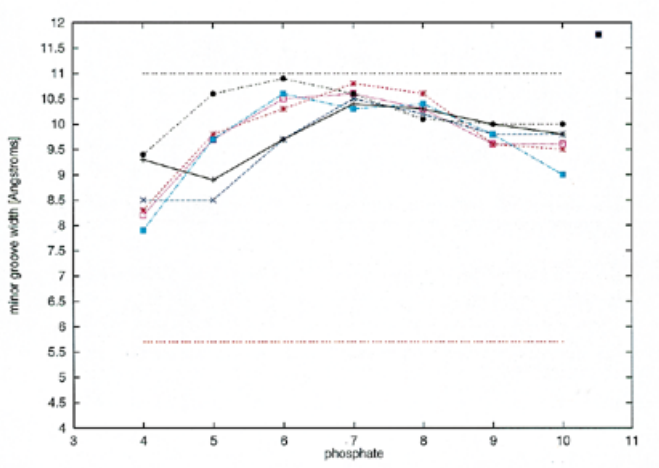

Figure 4. Comparison of the minor groove widths as measured for the r(GAAGAGAAGC)·d(GCTTCTCTTC) double helix (thick black line) and several A-DNA duplexes found in the NDB (accession nos uhj055 shown in blue, adj049 in red, adj055 in magenta, adj067 in cyan and ahj040 shown as black circles). Canonical A- and B-form DNA values are shown as black and orange dashed lines respectively.

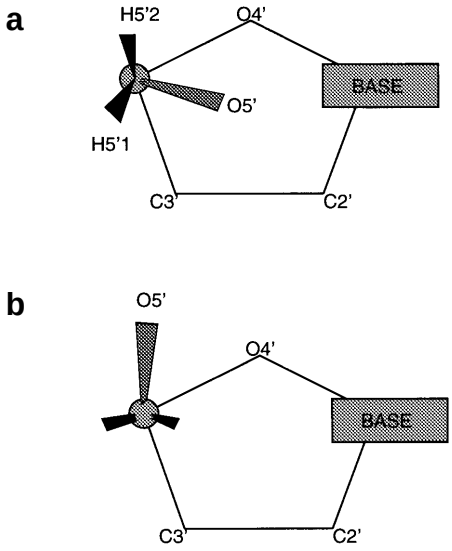

Figure 5. The sugar–phosphate backbone conformation resulting from αβγ *gtg* (**a**) and *ttt* (**b**) backbone torsion angles.

gives a schematic representation of the three-dimensional structure of the enzyme). The changes in chemical shift for these latter residues have been interpreted as resulting from conformational change in this part of the enzyme. Somewhat smaller chemical shift changes, also indicative of a modification of the conformation of the enzyme, were also observed for residues in a flexible loop region in the structure of the enzyme containing the conserved residues His124 and Asn130. His124 has been implicated in the catalytic function of RNase H (36). As it has also been pointed out that the flexibility of this loop is important as regards enzyme activity (36,37) it is not inconceivable that a change in the conformation of this loop might allow the enzyme to interact with a duplex of the type we have observed. In complementary experiments to the monitoring of NMR chemical shift changes in the enzyme upon duplex binding, Oda *et al.* (34) also monitored changes to the CD spectra of RNA/DNA hybrids on binding to the enzyme. These clearly indicate changes in the conformation of the duplexes on binding with blue shifts in the positions of the absorption maxima (263–258 nm), the appearance of new minima at 288 nm and changes in the form of the spectra in the region 210–240 nm. According to the authors of this study, these changes in the CD spectra suggest a bending of RNA/DNA duplexes upon binding to the enzyme while also allowing the possibility that their *global* conformation is also changed. Assuming that the structure of the duplexes studied by Oda *et al.* (34) in solution is the intermediate one described above for other RNA/DNA hybrids in solution, it appears possible that they do not have the same conformation when bound to RNase H. This thus raises the possibility that the global conformation we have observed for a hybrid in this crystal structure could be the one adopted when hybrids bind to RNase H. It is likely that the energy difference between the intermediate conformation observed in solution and the A′-form helix found in our crystal structure is small. Thus, the crystal structure may represent a 'snapshot' of one possible structure in the equilibrium of conformations found in solution. The present crystal structure can therefore add some further facets to the model of RNase H action, specifically how it achieves the observed substrate specificity. The alternating *gtg*/*ttt* conformation of the backbone of the RNA strand coupled with compression/extension of the P–P distances on the same strand provide an excellent mechanism for discriminating the two strands in a RNA/DNA hybrid duplex. Importantly, they would also allow RNase H to discriminate between RNA/DNA and pure RNA duplexes.

While it is not clear what the exact *in vivo* state of a hybrid duplex is when bound to RNase H, it is important to address the question of why the crystal structure should differ significantly from that found in solution. Rich and co-workers (5,6) have attributed the almost standard A-form structure of Okazaki fragments in the crystal to the strong preference for a C3′-*endo* conformation of the RNA residues. In essence, the DNA sugars on the RNA-containing strand are forced to adopt a similar conformation. However, studies of the same and other Okazaki fragments in solution (38,39) show that the pure DNA part of the duplex is essentially B-form while the hybrid part adopts an intermediate conformation similar to that seen in the solution structures of the 'pure' RNA/DNA hybrids discussed here. The authors of the solution studies ascribe the 'standard' A-form observed in the crystal structure to the effect of the crystallisation conditions and not to the influence of the RNA nucleotides. High concentrations of salts or precipitants (such as MPD or PEG) which cause a partial dehydration of the duplex may favour the adoption of a C3′-*endo* sugar conformation for both the ribose and deoxyribose groups (40) and similar arguments can be used to explain the differences between the solution and crystal structures of the hybrid under discussion here. It is thus likely that the conformation of the RNA/DNA hybrid in the crystal results from the influence of crystallisation conditions and the crystal structure would therefore appear to represent an alternative conformation for the hybrid that is more stable under conditions of low water activity. As discussed above, however, this does not neccesarily mean that the conformation we observe in the crystal is not biologically relevant.

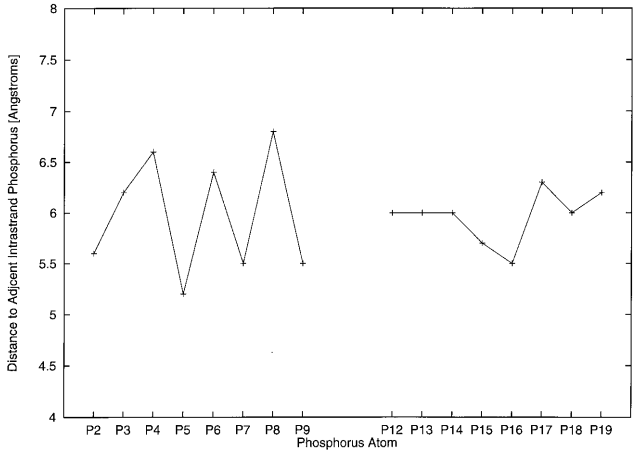

Figure 6. A plot of the distance between adjacent phosphorous atoms for the RNA (left) and the DNA (right) strands. From the P(4)–P(5) distance, there is a systematic alternating elongation and compression of P–P distances in the RNA strand.

Clearly, the crystal structure of the RNA/DNA hybrid r(GAAGAGAAGC)·d(GCTTCTCTTC) provides some intriguing new possibilities for a model of RNase H activity and specificity, particularly with respect to the conformation of the backbone of the RNA strand. However, the question still remains: are these regular alterations in backbone configuration we observe a general feature of RNA/DNA hybrids, crucially involved in hybrid recognition by RNase H, or are they an artifact of this particular sequence and set of crystallisation conditions? Only the three-dimensional structure of a RNase H–hybrid complex is likely to provide the final answer to this question.

ACKNOWLEDGEMENTS

This work was supported by the Medical Research Council of the UK, OSWEL Research Products Ltd and a Royal Society of Edinburgh Caledonian Research Fellowship to G.C. The authors would also like to thank Andrew Thompson and Vivian Stojanoff for help with the data collection and processing, Drs William Hunter and Andrew Lane for their encouragement and critical reading of the manuscript and Dr Sean McSweeney for help in the preparation of Figures 1 and 2.

REFERENCES

1 Hansen,U.M. and McClure,W.R. (1980) *J. Biol. Chem.*, **255**, 9564–9570.
2 Adams,R.L.P., Burdon,R.H., Campbell,A.M., Leader,D.P. and Smellie,R.M.S. (1981) *The Biochemistry of the Nucleic Acids*, 9th Edn. Chapman and Hall, London, UK, Chapter 6.
3 Stein,C.A. and Cheng,Y.-C. (1993) *Science*, **261**, 1004–1012.
4 Stein,H. and Hausen,P. (1969) *Science*, **166**, 393–395.
5 Egli,M., Usman,N., Zhang,S. and Rich,A. (1992) *Proc. Natl Acad. Sci. USA*, **89**, 534–538.
6 Egli,M., Usman,N. and Rich,A. (1993) *Biochemistry*, **32**, 3221–3237.
7 Gyi,J.I., Conn,G.L., Lane,A.N. and Brown T. (1996) *Biochemistry*, **35**, 4969–4982.
8 Gyi,J.I., Lane,A.N., Conn,G.L. and Brown T. (1998) *Biochemistry*, **37**, 73–80.
9 Fedoroff,O.Y., Salazar,M. and Reid B.R. (1993) *J. Mol. Biol.*, **233**, 509–523.
10 Lane,A.N., Ebel,S. and Brown,T. (1993) *Eur. J. Biochem.*, **215**, 297–306.
11 Salazar,M., Fedoroff,O.Y., Miller,J.M, Ribeiro,N.S. and Reid,B.R. (1993) *Biochemistry*, **32**, 4207–4215.
12 Gonzalez,C., Stec,W., Reynolds,M.A. and James T.L. (1995) *Biochemistry*, **34**, 4969–4982.
13 Fedoroff,O.Y., Ge,Y. and Reid,B.R. (1997) *J. Mol. Biol.*, **269**, 225–239.
14 Ratmeyer,L., Vinayak,R., Zhong,Y.Y., Zon,G. and Wilson,W.D. (1994) *Biochemistry*, **33**, 5298–5304.
15 Hung,S.-H., Yu,Q., Gray,D.M. and Ratliff,R.L. (1994) *Nucleic Acids Res.*, **22**, 4326–4334.
16 Wang,S.H. and Kool,E.T. (1995) *Biochemistry*, **34**, 4125–4132.
17 Lesnik,E.A. and Freier,S.M. (1995) *Biochemistry*, **34**, 10807–10815.
18 Sutton,D.H., Conn,G.L., Brown,T. and Lane,A.N. (1997) *Biochem. J.*, **321**, 481–486.
19 Scott,W.G., Finch,J.T., Grufnell,R., Fogg,J., Smith,T., Gait,M.J. and Klug,A. (1995) *J. Mol. Biol.*, **250**, 327–332.
20 Otwinowski,Z. and Minor,W. (1997) *Methods Enzymol.*, **276**, 307–326.
21 Berman,H.M., Olson,W.K., Beveridge,D.L., Westbrook,J., Gelbin,A., Demeny,T., Hsieh,S.-H., Srinivasan,A.R. and Scneider,B. (1992) *Biophys. J.*, **63**, 751–759.
22 Ramakrishnan,B. and Sundaralingham,M. (1993) *J. Mol. Biol.*, **231**, 431–444.
23 Rabinovitch,D. and Shakked,Z. (1984) *Acta. Crystallogr.*, A40, 195–200.
24 Brunger,A.T. (1992) *Nature*, **355**, 472–475.
25 Brunger,A.T. (1992) *X-PLOR Version 3.1: A System for Crystallography and NMR*. Yale University Press, New Haven, CT.
26 Parkinson,G., Vojtechovsky,J., Clowney,L., Brunger,A. and Berman,H.M. (1996) *Acta. Crystallogr.*, **D52**, 57–64.
27 Murshudov,G.N., Vagin,A.A. and Dodson,E.J. (1997) *Acta. Crystallogr.*, D53, 240–255.
28 Zimmerman,S.B. and Pheiffer,B.H. (1981) *Proc. Natl Acad. Sci. USA*, **78**, 78–82.
29 Saenger,W. (1984) *The Principles of Nucleic Acid Structure*. Springer-Verlag, New York, NY.
30 Weisz,K., Shafer,R.H., Egan,W. and James,T.L. (1994) *Biochemistry*, **33**, 354–366.
31 Sangahni,S.R. and Lavery,R. (1994) *Nucleic Acids Res.*, **22**, 1444–1449.
32 Dock-Bregeon,A.C., Chevrier,B., Podjarny,A., Johnson,J., de Bear J.S., Gough,G.R., Gilham,P.T. and Moras,D. (1989) *J. Mol. Biol.*, **209**, 459–463.
33 Wyatt,J.R. and Walker,G.T. (1989) *Nucleic Acids Res.*, **17**, 7833–7847.
34 Oda,Y., Iwai,S., Ohtsuka,E., Ishikawa,M., Ikehara,M. and Nakamura,H. (1993) *Nucleic Acids Res.*, **21**, 4690–4695.
35 Kanaya,S. and Ikehara,M. (1995) In Biswas,B.B. and Siddharta,R. (eds), *Subcellular Biochemistry, Vol. 24. Proteins: Structure Function and Engineering*. Plenum Press, New York, NY.
36 Oda,Y., Yoshida,M. and Kayana,S. (1993) *J. Biol. Chem.*, **268**, 88–92.
37 Morikawa,K. and Katayanagi,K. (1992) *Bull. Inst. Pasteur*, **90**, 71–82.
38 Salazar,M., Champoux,J.J. and Reid,B.R. (1993) *Biochemistry*, **32**, 739–744.
39 Salazar,M., Fedoroff,O.Y., Zhu,L. and Reid,B.R. (1993) *J. Mol. Biol.*, **241**, 440–445.
40 Saenger,W., Hunter,W.N. and Kennard,O. (1986) *Nature*, **324**, 385–388.